Electron Transport Properties in Novel Orthorhombically-strained Silicon Material Explored by the Monte Carlo Method

Xin Wang, D. L. Kencke, K. C. Liu, A. F. Tasch, Jr., L. F. Register and S. K. Banerjee

Microelectronics Research Center, The University of Texas at Austin,
R9950, Austin,TX 78758. Email: xwang3@ece.utexas.edu.

Abstract--We report for the first time on the electron transport properties of simple orthorhombically-strained silicon studied by density-functional theory and Monte Carlo simulation. The six degenerate valleys near X points in bulk silicon break into three pairs with different energy minima due to the orthorhombic strain. The degeneracy lifting causes electron redistribution among these valleys at low and intermediate electric fields. Thus the drift velocity is enhanced under an electric field transverse to the long-axis of the lowest valleys. The simple orthorhombically-strained Si grown on a $Si_{0.6}Ge_{0.4}$ sidewall has a low-field mobility almost twice that of bulk Si and an electron saturation velocity approximately 20% higher.

INTRODUCTION

The development of vertical MOSFET's introduces to a orthorhombically-strained silicon (OS-Si) channel pseudomorphically grown as a sidewall on the edge of a compressively-strained SiGe (CS-SiGe) pillar [1]. In the vertical silicon sidewall device, the bulk silicon substrate defines the dimensions of a strained $Si_{1-x}Ge_x$ layer grown on it, and subsequently the strained $Si_{1-x}Ge_x$ lattice determines the shape of the OS-Si sidewall (Fig. 1). It is surmised that this sidewall Si material becomes deformed into a simple orthorhombic lattice. All three dimensions of the unit cell are different from each other in length since the SiGe base on which the material grows is a rectangle with one side that conforms to the substrate Si lattice constant and one side that is elongated according to the Poisson ratio to accommodate the SiGe alloy pseudomorphically. The third dimension is determined as the Si cap material grows, and like biaxially tensily-strained tetragonal Si, the Si sidewall should have a lattice constant in the growth direction that is less than the lattice constant of cubic Si. However, unlike tensily-strained Si, all three <100> dimensions of the OS-Si unit cell are of different lengths.

Orthorhombic strain breaks the symmetry of the unit cell of bulk Si and separates degenerate states. This new band structure provides different electronic transport properties for vertical silicon n-MOSFET's. In this paper, we report the unique electronic properties of OS-Si studied by density-functional theory (DFT) and the Monte Carlo (MC) method.

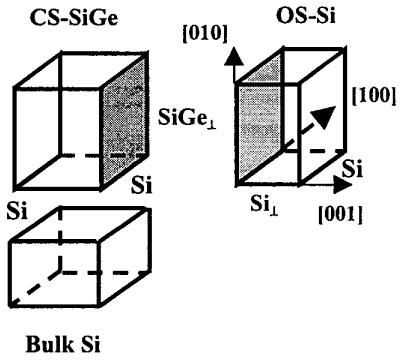

Fig. 1. Unit cells of bulk Si, CS-$Si_{1-x}Ge_x$ and OS-Si.

THEORETICAL MODELS

The electronic properties of OS-Si are a function of the atomic positions in a strained unit cell. We assume the two interfaces, $Si_{1-x}Ge_x$/Si substrate and OS-Si/$Si_{1-x}Ge_x$ are lattice-matched with no dislocations across the interfaces. Thus the in-plane lattice constants are the same across the interfaces. The normal lattice constants can be determined by minimizing the macroscopic elastic energy [2].

The band structure of OS-Si is calculated by a well-tested DFT package [3] which self-consistently solves the Kohn-Sham equation [4]. The electron exchange correlation is treated by a local-density approximation [4], and non-local norm-conserving pseudopotentials [5] in the fully separable Kleinman-Bylander form [6] describe the electron-nuclei interaction. Electron waves are expanded in terms of plane waves, the number of which is determined by the energy cutoff, 30 Ry. Integration in momentum space is approximated by a weighted summation of 16 special k-points in the irreducible Brillouin zone.

For a study of the transport properties, we run a hybrid MC code, SLAPSHOT0D [7], on a fine mesh with even spacing $0.025(2\pi/a)$, a being the lattice constant of bulk silicon. The strain-split full band structure is used for generating a scattering rate look-up table for choosing the

0-7803-6279-9/00/$10.00 © 2000 IEEE

scattering type. For electron free-flight and post-scattering momentum selection processes, we use a set of nonparabolic bands

$$E(k)[1+\alpha E(k)]=\frac{1}{2}\left(\frac{h}{2\pi}\right)^2\sum_{i=1}^{3}\frac{k_i^2}{m_i}, \qquad (1)$$

where α is the nonparabolicity and m_i is the electron effective mass in the principal direction i. These parameters are obtained by fitting both the $E(k)$ relations in the principal crystal directions and density of states (DOS) extracted from real bands. For OS-Si, we found the effective masses, longitudinal and transverse, are essentially same as those of bulk Si.

We consider electron-phonon scattering, electron-impurity scattering and impact ionization in this simulation of bulk properties. In the electron-phonon scattering formula, the deformation potentials, Δ_{LA}, Δ_{TA} (acoustic phonon) and DK_{op} (optical phonon), are adjusted to fit the experimental velocity-field characteristics [8] of bulk Si at 300K. A set of the deformation potentials is found:

$$\Delta_{LA}=\Delta_{TA}=\begin{cases}1.3\,eV\,(1st\ band)\\0.9\,eV\,(2nd\ band),\\0.7\,eV\,(3rd\ band)\end{cases} \qquad (2)$$

$$DK_{op}=\begin{cases}4.2\times10^{8}\,eVcm^{-1}\,(1st\ band)\\3.7\times10^{8}\,eVcm^{-1}\,(2nd\ band).\\3.5\times10^{8}\,eVcm^{-1}\,(3rd\ band)\end{cases} \qquad (3)$$

The electron-ionized impurity scattering is implemented using the traditional Brooks-Herring formula [9]. A multi-threshold energy formula [10] is used for impact ionization with $E_{gap}=1.1-0.585x$ extracted from the results of Ref. 1.

SIMULATION RESULTS AND DISCUSSION

Figure 2 shows the changes of lattice constants of OS-Si with mole fraction x. Under the constraint of the bulk Si substrate, the [100] lattice constant of the SiGe pillar and, thus the OS-Si layer remains the same as for bulk Si, while in the [010] direction the lattice of OS-Si is enlarged to conform to the extended side of the compressively strained $Si_{1-x}Ge_x$ pillar. The lattice spacing in [001] is compressed to minimize the elastic energy coming from the tensile [010] strain.

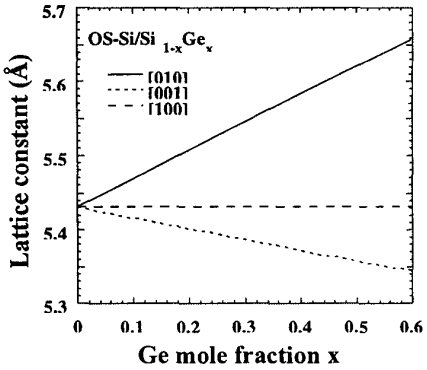

Fig. 2. Lattice constants of OS-Si for various mole fractions of Ge in the $Si_{1-x}Ge_x$ layer.

The strain in OS-Si breaks the six-fold degenerate Δ valleys near X points into three pairs (Fig. 3 and Fig. 4). Two-fold degenerate tensily-strained [010] valleys move up; compressively-strained [001] valleys move down; and the third pair, for which the [100] lattice constant is the same as that of bulk Si, only experiences hydrostatic strain and moves up a little because of a positive hydrostatic deformation potential for Si. The shear and hydrostatic deformation potentials [11], extracted from the energy shift and splitting for Δ valleys are 8.75 eV and 4.3 eV, respectively.

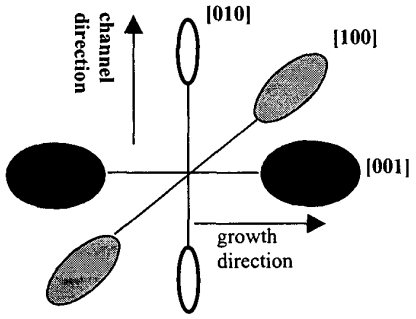

Fig. 3. Schematic equi-energy surfaces of the six split Δ valleys.

Figure 5 shows the DOS of OS-Si, calculated from the full band structure. We see the valley splitting broadens and lowers the DOS peaks, but the band structure remains predominantly Si-like.

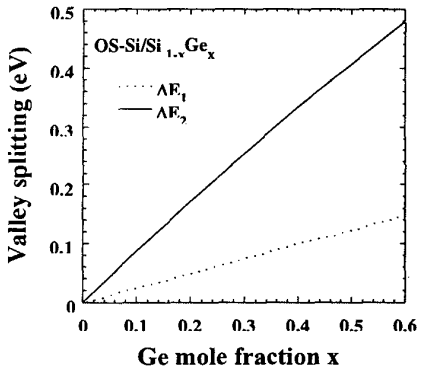

Fig. 4. Δ valley splitting in a sidewall OS-Si as a function of Ge mole fraction. $\Delta E_1=E_{[100]}-E_{[001]}$ and $\Delta E_2=E_{[010]}-E_{[001]}$. $E_{[001]}$ refers to the minimum of $\Delta_{[001]}$ valley.

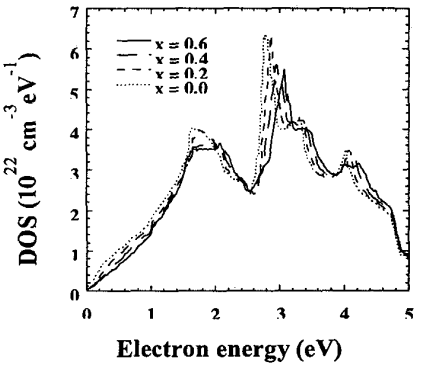

Fig. 5. Conduction band density of states for bulk Si and OS-Si grown on $Si_{1-x}Ge_x$ sidewalls.

In this paper, we only consider the electron transport properties of OS-Si at low doping concentration, 10^{18} cm^{-3} at 300 K. Figure 6 shows the electron occupancies in the Δ valleys for OS-Si on $Si_{0.8}Ge_{0.2}$ as a function of fields applied along [010] and [100] directions. Due to the valley splitting, at low fields most of electrons occupy the $\Delta_{[001]}$ valleys which are lowest in energy. The $\Delta_{[100]}$ valleys are less preferred, while the higher $\Delta_{[010]}$ valleys are essentially empty. With the increase of field strength, more electrons move up to the high-energy valleys, $\Delta_{[100]}$ and $\Delta_{[010]}$ until they are almost evenly distributed among the Δ valleys at very high fields. We note that at high fields, the total occupancy of the Δ valleys also drops as electrons reach the higher-lying valleys.

Figure 7 exhibits the electron drift velocity for [100], [001] and [001] field orintations for OS-Si on $Si_{0.8}Ge_{0.2}$. Because most electrons occupy $\Delta_{[001]}$ valleys at low fields, they have the smaller effective mass component m_t parallel to the field for either the [100] or [010]-oriented fields. Consequently, the drift velocities are comparable for these two field orientations. At intermediate fields, however, the relative increase in electron concentration in the $\Delta_{[100]}$ valley leads to some splitting of the drift velocities. Electrons in the $\Delta_{[100]}$ valleys have the heavier mass component m_l along the [100] field direction. For [001]-oriented fields, on the other hand, most electrons have the heavier mass component m_l parallel to the field for low and intermediate fields. This heavier mass results in much lower drift velocities for [001] field orientation than for either [100] or [010] field orientations. At high fields where the carriers are more evenly distributed among the valleys, the average energies converge and the drift velocities merge to a saturation velocity of approximately $1.2X10^7$ cm/s.

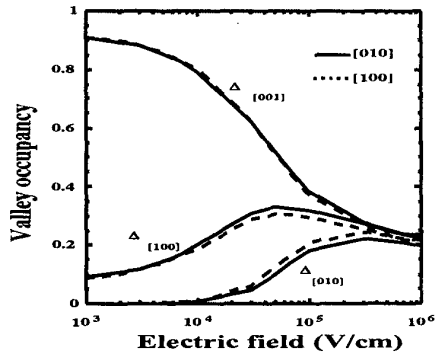

Fig. 6. Electron distribution among Δ valleys for OS-Si grown on a $Si_{0.8}Ge_{0.2}$ sidewall as a function of electric field along [010] and [100].

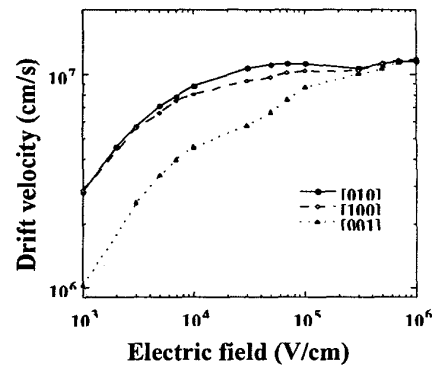

Fig. 7. Electron drift velocities for OS-Si grown on a $Si_{0.8}Ge_{0.2}$ sidewall as a function of electric field.

In the vertical n-MOSFET, the channel is along the [010] direction. In Fig.8, the drift velocities are compared for various Ge mole fractions in $Si_{1-x}Ge_x$, x=0.1, 0.2, 0.4 and 0.6, on which OS-Si sidewall is grown. Increasing Ge mole fraction produces more valley splitting and, thus, more electrons reside in the $\Delta_{[001]}$ valleys, where the electron effective mass parallel to the field is the lighter value m_t. Valley splitting also suppresses the f-type intervalley scattering among neighboring Δ valleys, causing drift velocities to increase with mole fraction at low and intermediate fields in OS-Si. Also the low-field electron mobility is enhanced in OS-Si. For instance, the mobility of OS-Si grown on $Si_{0.6}Ge_{0.4}$ can be twice as large as that of bulk Si.

CONCLUSIONS

In this paper, we presented a comprehensive theoretical investigation of electron transport in OS-Si that is produced when Si is grown on the sidewall of a $Si_{1-x}Ge_x$ epitaxial mesa structure for application in a vertical MOSFET. The uniaxial strain splits the degenerate valleys and changes the electron occupancy among the valleys, with most electrons occupying the lowest pair of valleys. For a transverse field along [010], most electrons have a small effective mass component. The mobility is enhanced along the channel direction of a vertical MOSFET more than a factor of two (for x=0.4) and a 20% higher saturation velocity can be obtained. Compared with conventional tensily-strained Si, OS-Si has comparable mobility and a higher saturation velocity that is important in deep-submicron devices.

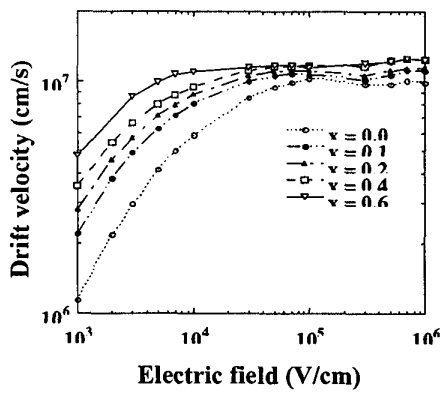

Fig. 8 Electron drift velocities for OS-Si grown on $Si_{1-x}Ge_x$ for fields along [010] for varying Ge mole fraction.

ACKNOWLEDGEMENTS

The authors thank D. R. Hamann for providing the computer code which calculates Si pseudopotentials. This work was supported in part by the Semiconductor Research Cooperation, NSF-STC and DOD-MURI.

REFERENCES

[1] K. C. Liu, X. Wang, E. Quinones, X. Chen, X. D. Chen, D. L. Kencke, B. Anantharam, R. D. Chang, S. K. Ray, S. K. Oswal, C. Y. Tu, and S. K. Banerjee, IEEE IEDM Tech. Dig., 63 (1999).

[2] C. G. Van de Walle and R. M. Martin, Phys. Rev. B **34**, 5621 (1986).

[3] M. Bockstedte, A. Kley, and M. Scheffler, Comp. Phys. Comm. **107**, 187 (1997).

[4] D. M. Ceperley and B. J. Alder, Phys. Rev. Lett. **45**, 567 (1980).

[5] G. B. Bachelet, D. R. Hamann, and M. Schluter, Phys. Rev. B **26**, 4199 (1982).

[6] L. Kleinman and D. M. Bylander, Phys. Rev. Lett. **48**, 1425 (1982).

[7] X. Wang, V. Chandramouli, C. M. Maziar, and Al F. Tasch, Jr., J. Appl. Phys. **73**, 3339 (1993).

[8] C. Canali, C. Jacoboni, F. Nava, G. Ottaviani, and A. Alberigi-Quaranta, Phys. Rev. B **12**, 2265 (1975).

[9] H. Brooks and C. Herring, Phys. Rev. **83**, 879 (1951).

[10] E. Cartier, M. V. Fischetti, E. A. Eklund, and F. R. McFeely, Appl. Phys. Lett. **62**, 3339 (1993).

[11] C. G. Van de Walle, Phys. Rev. B **39**, 1871 (1989).